Journal of Clinical Neuroscience 141 (2025) 111562

Contents lists available at ScienceDirect

Journal of Clinical Neuroscience

journal homepage: www.journals.elsevier.com/journal-of-clinical-neuroscience

Original Research

The vascular safe zone for endoscopic third ventriculostomy: a radiomorphometric study

Nicolás Rincón-Arias [a,b,*], Nadin J. Abdala-Vargas [c], Sabino Luzzi [d], Julián D. Barraza [a,b], Luisa Fernanda Jaimes [e], Pablo Baquero [b], Matias Baldoncini [f], Álvaro Campero [g], Daniela Martínez Laverde [h], Edgar G. Ordoñez-Rubiano [a,i], Hernando A. Cifuentes-Lobelo [b]

[a] Department of Neurosurgery, Fundación Universitaria de Ciencias de la Salud – FUCS, Hospital de San José – Sociedad de Cirugía de Bogotá, Bogotá, Colombia
[b] Department of Neurosurgery, Fundación Universitaria de Ciencias de la Salud – FUCS, Hospital Infantil Universitario de San José, Bogotá, Colombia
[c] Department of Neurosurgery, La Misericordia Clínica Internacional. Barranquilla, Colombia
[d] Department of Neurosurgery, Università di Pavia, Lombardy, Italy
[e] Department of Neuroradiology, Fundación Universitaria de Ciencias de la Salud – FUCS, Hospital Infantil Universitario de San José, Bogotá, Colombia
[f] Department of Neurological Surgery, Sanatorio Mater Dei Sagrada Familia, Buenos Aires, Argentina
[g] Department of Neurosurgery, Jefe de Servicio de Neurocirugía del Hospital Padilla, Tucumán, Argentina
[h] Fundación Instituto Neurológico de Colombia, Medellín, Colombia
[i] Department of Neurosurgery, Hospital Universitario Fundación Santa Fe de Bogotá, Bogotá, Colombia

ARTICLE INFO

Keywords:
Endoscopic third ventriculostomy
Third ventricle floor
Hydrocephalus
Neuroendoscopy
Basilar artery complex
Neurosurgery

ABSTRACT

Background and objective: Endoscopic third ventriculostomy (ETV) is a minimally invasive procedure for hydrocephalus management. Variable neuroanatomical features in the floor of the third ventricle (3VF) and the basilar artery (BA) complex contribute to the risk of vascular lesions in the BA complex. This study aims to evaluate the neuroradiological characteristics of the 3VF with the BA complex to determine the ETV fenestration "vascular safe zone".

Methods: Preoperative neuroimaging studies from a consecutive cohort of adult patients who underwent ETV between January 2016 and March 2025 were retrospectively reviewed. Preoperative MRIs were used to evaluate the neuroradiological axial and sagittal characteristics of the 3VF with the BA complex.

Results: The neuroradiological BA complex position was described. In the sagittal plane, Type II (74 %) was the most common, with mean distances ranging from 4.1 mm to 8 mm. The mean distance from the top of the BA complex to the 3VF was 6.86 mm (SD 1.56 mm). In the axial plane, Classes C and D (71.2 %) were predominant and had varied distances to the 3VF.

Conclusions: Our results suggest that the "vascular safe zone" for an ETV fenestration is primarily located in the anterior half of the 3VF. 71.2 % of our cases showed that the basilar artery (BA) complex was located in the posterior half. Future research should validate the "vascular safe zone" for ETV fenestration with neuroendoscopy intraoperative observations and assess clinical outcomes, including post-operative complications and success rates, to ensure the effectiveness of the proposed fenestration area.

1. Introduction

Endoscopic third ventriculostomy (ETV) is a minimally invasive procedure used in both obstructive and non-obstructive hydrocephalus. It serves as an alternative procedure to shunt operations by offering a more "physiological" restoration of cerebrospinal fluid (CSF) flow [1–4]. Indications for ETV must account for the variable neuroanatomical characteristics of each case, as the procedure involves creating a stoma on the floor of the third ventricle (3VF). This stoma allows for the drainage of CSF from the third ventricle into the interpeduncular and prepontine cisterns [5,6] (see Fig. 1).

The 3VF is a complex anatomical region with several structures and variable neuroanatomical characteristics. The 3VF is a thin and translucent structure associated with fenestration in the ETV. Anatomically,

Abbreviations: BA, Basilar artery; ETV, Endoscopic third ventriculostomy; 3VF, Third ventricle floor; CSF, cerebrospinal fluid.

* Corresponding author at: Neurosurgery Resident. Department of Neurosurgery, Hospital de San José, Calle 10 # 18-75, 110111 Bogotá, Colombia.
E-mail address: nrincon@fucsalud.edu.co (N. Rincón-Arias).

https://doi.org/10.1016/j.jocn.2025.111562
Received 10 June 2025; Accepted 12 August 2025

from anterior to posterior, we find the optic chiasm, the infundibular recess, the tuber cinereum, the mammillary bodies, and the posterior perforated substance [7]. Laterally, the 3 V is surrounded by the hypothalamic sulci, and on its floor, the basilar artery (BA) complex is located [8,9].

The floor of the 3 V extends from the optic chiasm anteriorly to the orifice of the aqueduct of Sylvius. The anterior half of the floor is comprised of the infundibulum of the hypothalamus, the tuber cinereum, and the mamillary bodies. In contrast, the posterior half includes the posterior perforated substance and part of the tegmentum [7].

The 3VF is avascular, a feature that is particularly relevant for surgical procedures as a safe entry zone. Notably, anatomical variations in the floor's thickness, translucency, and configuration are common, especially in patients with hydrocephalus, and influence the neurosurgical planning and neurovascular risk assessment [7,10] (see Fig. 2).

The long-term success rate of the ETV varies between 50 % and 80 % [11,12]. However, iatrogenic BA complex lesions occur within 0.5 % to 3.9 % of ETV cases [13–16]. Some of these complications include 1) vascular lesions, 2) oculomotor injuries, 3) hypothalamic injuries, and 4) fornix injuries [13–16]. However, the actual incidence remains unknown.

The variability of the BA complex and the 3VF in each case has not been thoroughly evaluated neuroradiologically in terms of precise neuroanatomical axial and sagittal positions. Therefore, determining the "vascular safe zone" for fenestration of the 3VF becomes a crucial consideration to reduce the risk of injury to the BA complex [17,18]. The present study aims to preoperatively determine the "vascular safe zones" for ETV fenestration, taking into account the patient's specific BA complex anatomical characteristics (see Fig. 3).

2. Methods

Preoperative neuroimaging studies of a consecutive cohort of adult (≥18 years old) patients who had undergone an ETV between January 1st, 2016, and March 29th, 2025, were retrospectively reviewed from the institutional neurosurgical database of Hospital Infantil Universitario de San José, Bogotá, Colombia.

Institutional Review Board approval was obtained from the Fundación Universitaria de Ciencias de la Salud – FUCS. This study was conducted in accordance with all principles outlined in the Declaration of Helsinki.

On the axial plane, the optic chiasm, mammillary bodies, and hypothalamus were used as landmarks to identify the surgical 3VF. Two lines were drawn: 1) Middle antero-posterior line from the optic chiasm to the mammillary bodies, and 2) Latero-lateral line from both hypothalamus, dividing the area into four quadrants, reported as Class A: left anterior, Class B: right anterior, Class C: left posterior, and Class D: right posterior. The axial location of the BA complex was classified into Classes A to D, accordingly (see Fig. 4).

On the sagittal plane, the distance between the 3VF and the top of the BA was measured, and three Types were identified: Type 1: ≤4 mm, Type 2: 4.1–8 mm, and Type 3 >8 mm.

2.1. Neuroradiological protocol to define the relation of the BA complex and the 3VF

Magnetic resonance imaging (MRI) was performed using a 1.5 T superconducting magnet (General Electric, Signa Creator). The study focused on preoperative brain axial and sagittal T2-weighted images, as well as T1 contrast-weighted images.

A Field of View (FOV) of 220 mm, Repetition Time (TR) of 9.3 ms, Echo Time (TE) of 3.6 ms, Inversion Time (TI) of 450 ms, Flip Angle (FA) of 12 degrees, Phase Direction (PHDIR) R/L, and Bandwidth (BW) of 130 Hz. An isovolumetric sequence (BRAVO) was applied, with acquisition in the sagittal plane, slice thickness of 1 mm, and reconstructions in the axial plane with Maximum Intensity Projection (MIP) at a thickness of 2 mm, without angulation. The focus was on the F3V to define the location and relation of the BA complex (see Fig. 5).

2.2. Statistical analysis

A descriptive analysis was conducted for quantitative variables, involving calculations of measures of central tendency (mean and median), dispersion (standard deviation and interquartile range [IQR]), and position. For qualitative variables, absolute and relative frequencies were determined. The test of difference of proportions between classes and types was also performed. Additionally, the Kruskal-Wallis test was used to assess potential differences in distribution and position among all classes, assuming a significance level of 0.05. All hypothesis tests considered an alpha of 0.05 and a confidence level of 95 %. The data analysis was carried out using R language version 4.3.

3. Results

Overall data from 250 adult cases were collected. The mean age of the patients was 51.2 years. The average distance (±SD) between the

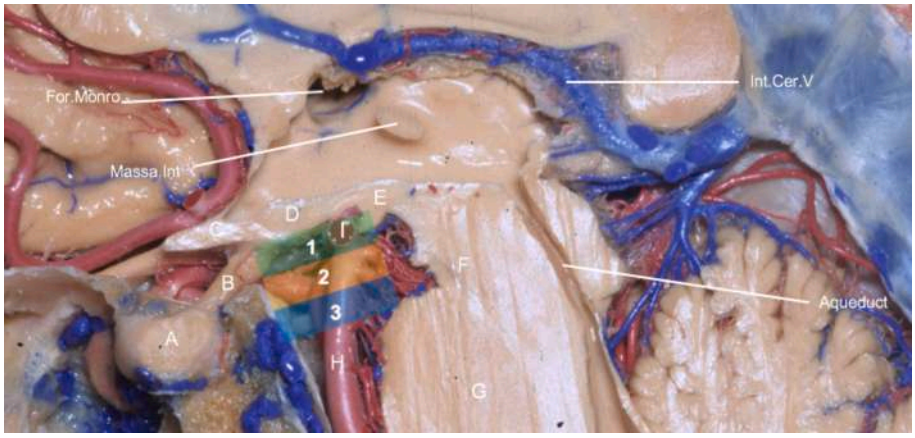

Fig. 1. Sagittal neuroanatomical section of the 3VF. Type I: Shaded in green; the top of the basilar artery is located at a distance ≤4 mm from the tuber cinereum. Type II: Shaded in yellow; the top of the basilar artery is located at a distance of 4.1–8 mm from the tuber cinereum. Type III: Shaded in blue; the top of the basilar artery is located at a distance >8 mm from the tuber cinereum. *a. Pituitary gland. b. Infundibular stalk. c. Optic chiasm. d. Tuber cinereum in the F3V. e. Mammillary body. f. Mesencephalon. g. Pons. h. Basilar artery. i. Basilar top.* (For interpretation of the references to colour in this figure legend, the reader is referred to the web version of this article.)

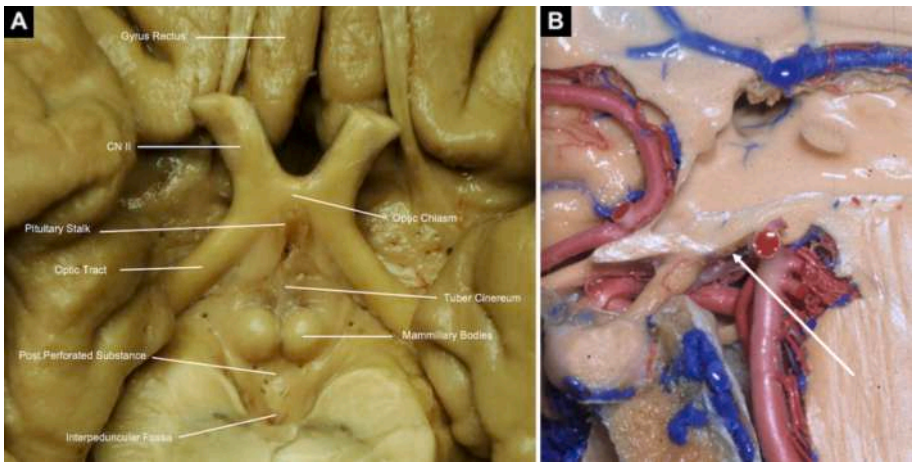

Fig. 2. 3VF neuroanatomical. (A) Inferior view. From front to back, there is the lower margin of the optic chiasm, the pituitary stalk, the tuber cinereum, the mammillary bodies, the posterior perforated substance and the midbrain. The yellow arrow delineates the "usual zone" where neuroendoscopic fenestration of the P3V is performed. (B) Sagittal neuroanatomical section where the white arrow indicates the view of the 3VF. (For interpretation of the references to colour in this figure legend, the reader is referred to the web version of this article.)

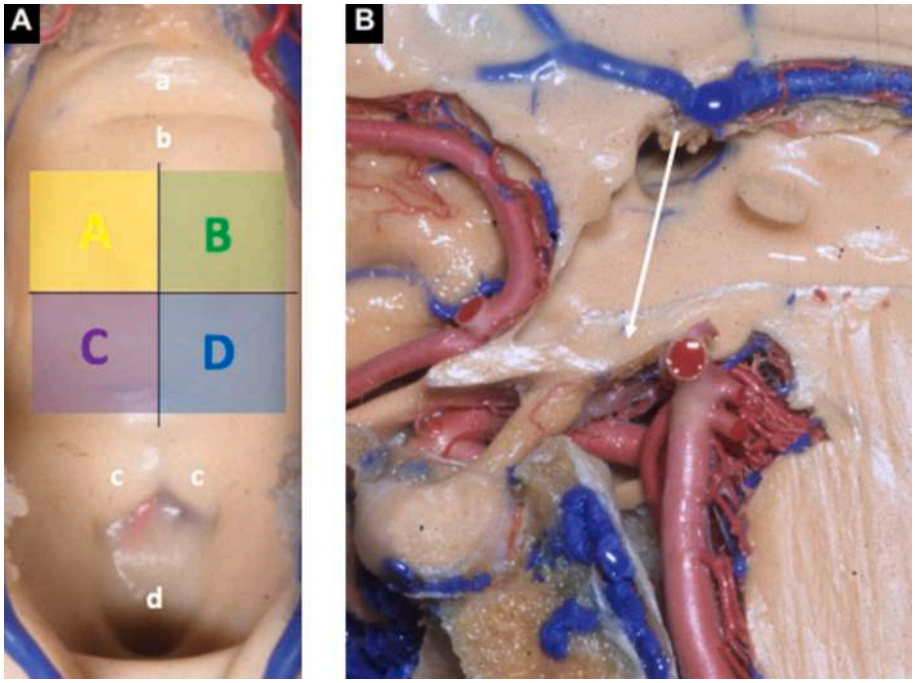

Fig. 3. (A) F3V neuroanatomical superior view. A: Shaded in yellow; the basilar artery complex is located anterior left in the tuber cinereum. B: Shaded in green; the basilar artery complex is located anterior right in the tuber cinereum. C: Shaded in purple; the basilar artery complex is located posterior left in the tuber cinereum. D: Shaded in blue; the basilar artery complex is located posterior right in the tuber cinereum. (B) Sagittal neuroanatomical section where the white arrow indicates the view from the foramen of Monro of the 3VF. *a. Optic chiasm. b. Infundibular recess. c. Mammillary bodies. d. Interpeduncular fossa.* (For interpretation of the references to colour in this figure legend, the reader is referred to the web version of this article.)

optic chiasm and the mammillary bodies was 7.36 (±1.6 mm). The average distance (±SD) between the hypothalamic walls as the lateral landmarks of the 3VF was 5.52 mm (±1.5 mm).

Regarding the axial plane classification, the BA complex was found in the Class A and B, that represents the anterior half, in 28.8 % of cases (72 cases), with a 95 % confidence interval (CI) of 0.34 to 0.51. Classes C and D, representing the posterior half, had 71.2 % of cases (178 cases). This difference was statistically significant ($p < 0.001$).

For the sagittal plane, the mean distance from the top of the BA complex to the 3VF was 6.86 mm (SD 1.56 mm). The BA complex was found at a distance of <4 mm from the 3VF (Type 1) in 18 patients (7.2 %). The distance ranged between 4.1 mm and 8 mm (Type 2) in 185 patients (74 %), and >8 mm (Type 3) in the remaining 47 patients (18.8 %). Table 1 summarizes the overall results of axial and sagittal plane classifications of the BA complex at the level of the 3VF.

The average distances and interquartile range (IQR) between the top of the BA and the 3VF in relation to the different axial plane classes, expressed as median distance, were:

- Class A: 6.85 mm (IQR of 5.35 to 7.4 mm);
- Class B: 6.50 mm (IQR of 5.4 to 7.8 mm);
- Class C: 6.80 mm (IQR of 5.8 to 7.7 mm);
- Class D: 6.80 mm (IQR of 5.9 to 7.68 mm).

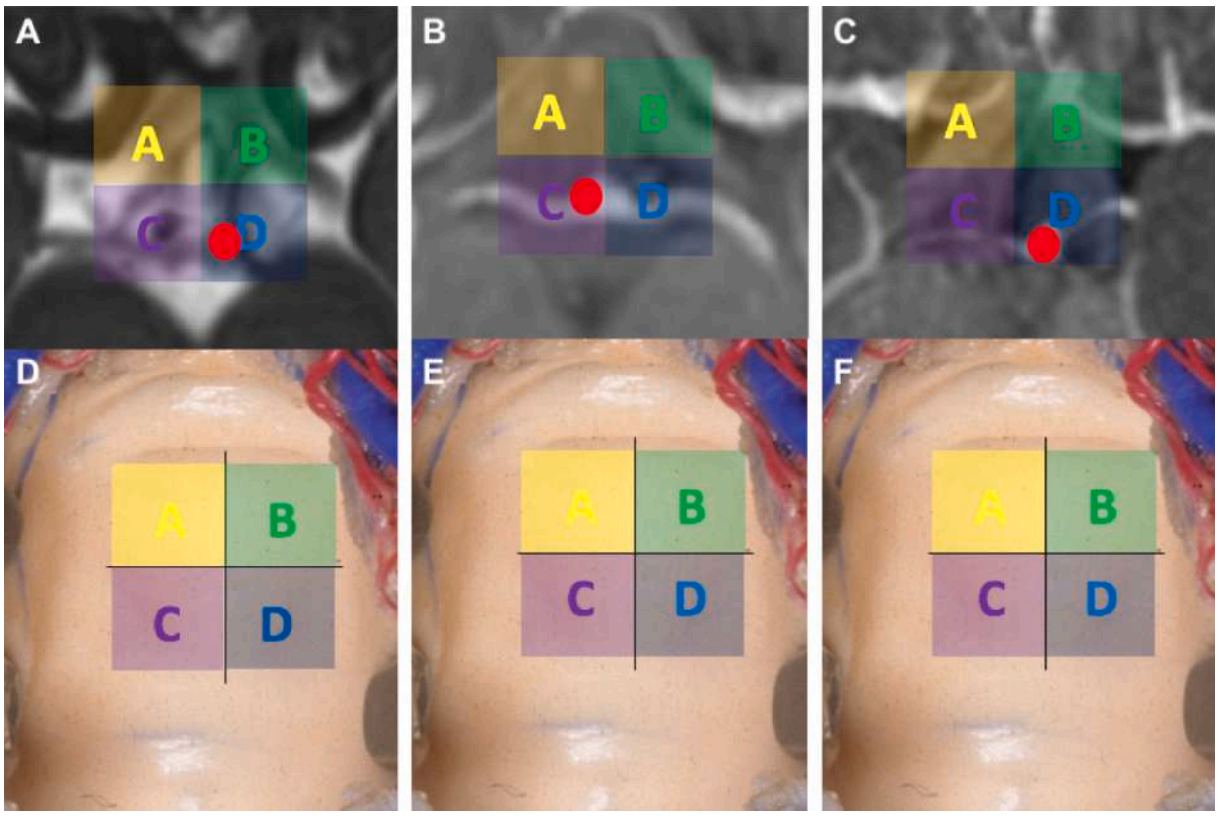

Fig. 4. Neuroradiological and neuroanatomical axial classification relations to the quadrants where the "safe zone" of fenestration of the 3VF can be located. Class A: Shaded in yellow. Class B: Shaded in green. Class C: Shaded in purple. Class D: Shaded in blue. The red dot in the upper images represents the location of the AB complex. (For interpretation of the references to colour in this figure legend, the reader is referred to the web version of this article.)

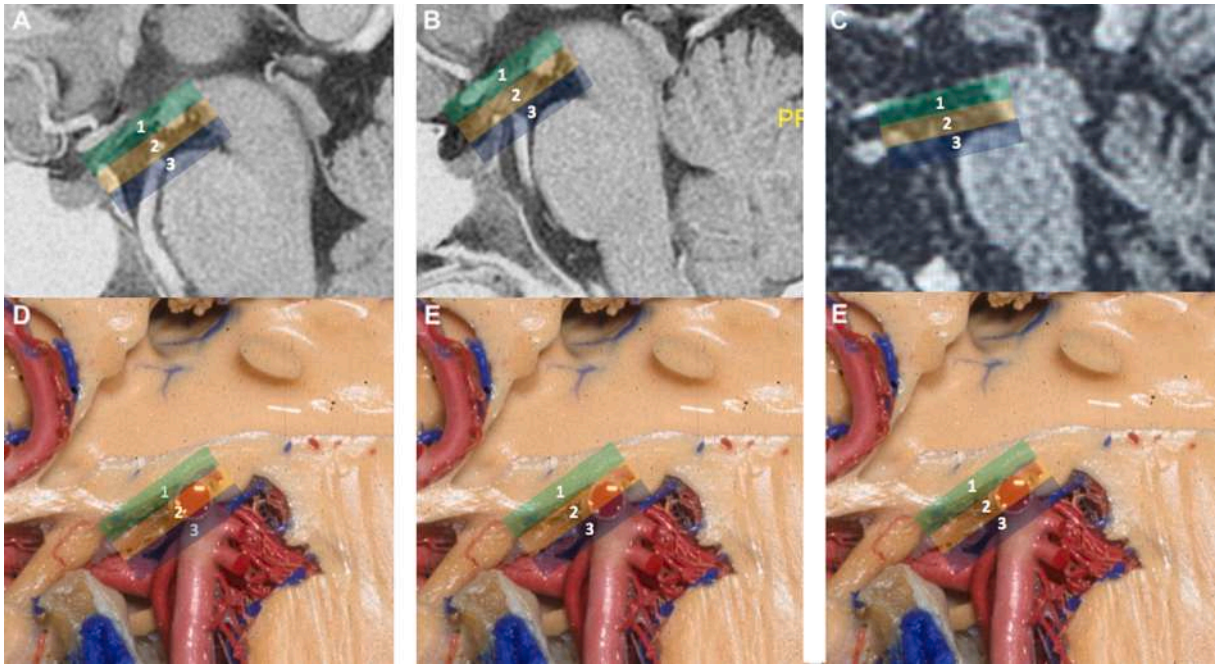

Fig. 5. Neuroradiological – neuroanatomical sagittal classification and relations of the distance from the top of the BA complex to the tuber cinereum. Type I: Shaded in green. Type II: Shaded in yellow. Type III: Shaded in blue. (For interpretation of the references to colour in this figure legend, the reader is referred to the web version of this article.)

These results indicate that the median distances between the top of the BA and the 3VF were similar across all cases, regardless of the axial plane classification ($p = 0.0.89$). Table 2 shows the distances between the top of the BA and the 3VF in relation to the different axial plane classifications.

The Pearson test analysis did not reveal a correlation between age

Table 1
Data of axial and sagittal plane measurements of BA complex in relation with the tuber cinereum at the level of the 3VF. The axial classification includes Classes A, B, C, and D, along with a breakdown of cases in the anterior and posterior halves of the 3VF. Additionally, the sagittal classification comprises Types I, II, and III, provide the position of the BA complex from the 3VF.

Parameter	Data		*p*-value
Axial plane measurements:			
Distance between optic chiasm and mammillary bodies – average mm (±SD)	7.36 (±1.6)	NA	
Distance between hypothalamic walls – average mm (±SD)	5.52 (±1.5)	NA	
Class A + B (anterior half) n. of cases (%)	72 (28.8 %)	CI 95 % (0.34–0.51)	<0.001
Class C + D (posterior half) n. of cases (%)	178 (71.2 %)		
Class A (left anterior) – n. of cases (%) vs Class B, C, D	40 (16 %)	CI 95 % (0.16–0.84)	<0.001
Class B (right anterior) – n. of cases (%) vs Class A,C,D	32 (12.8 %)	CI 95 % (0.12–0.87)	<0.001
Class C (left posterior) – n. of cases (%) vs Class A, B, D	88 (35.2 %)	CI 95 % (0.20–0.38)	<0.001
Class D (right posterior) – n. of cases (%) vs Class A, B, C	90 (36 %)	CI 95 % (0.19–0.36)	<0.001
Sagittal plane measurements:			
Type I – n. of cases (%) vs Type II, III	18 (7.2 %)	CI 95 % (−0.9 –(−0.8))	<0.001
Type II – n. of cases (%) vs Type I, III	185 (74 %)	CI 95 % (0.39–0.56)	<0.001
Type III – n. of cases (%) vs Type I, II	47 (18.8 %)	CI 95 % (0.55–0.69)	<0.001

BA: basilar artery; NA: not applicable.

Table 2
Distances between the top of the BA complex and 3VF in relation to the different axial plane classes.

Axial plane class	Data	*p*-value
Class A – median mm (IQR)	6.85 (5.35–7.4)	0.89
Class B – median mm (IQR)	6.50 (5.4–7.8)	
Class C – median mm (IQR)	6.80 (5.8–7.7)	
Class D – median mm (IQR)	6.80 (5.9–7.68)	

BA: basilar artery; 3VF: third ventricle floor; IQR: Interquartile Range.

and the distances from the top of the BA to the 3VF (R = −0.168).

4. Discussion

ETV is a well-established procedure for treating both obstructive and non-obstructive hydrocephalus. Preoperative neuroradiological assessment is essential for evaluating neuroanatomical details, including the size of the lateral ventricles, the dimensions of the foramen of Monro, the length and width of the 3VF, and the BA complex location in relation to the 3VF [19]. The iatrogenic BA complex lesions can be prevented by ensuring that the ETV fenestration is in the correct position, which, based on our cohort, will be located in the anterior aspect of the 3VF in at least 71 % of the cases. A presurgical, thoughtful analysis should be performed in each specific case.

Anatomical variations in the BA complex and the 3VF have been documented [20,21]. Careful evaluation and knowledge of the localization of the BA complex are essential for improving intraoperative management. Although "standard" ETV is used in most cases, a modified technique can be required based on the axial and sagittal position of the BA complex to avoid iatrogenic vascular complications [6,19]. Some authors consider a "standard central" zone within the 3VF as the "standard" ETV fenestration zone [17,18]. According to Schmidt et al., the BA complex's usual location is anterior to the mammillary bodies [11]. In contrast, Ram Yadav et al. describe the ETV as being anterior to the BA and in the midline of the 3VF [19]. The concept of a "vascular safe zone" for ETV cannot be applied universally to all cases, and it does not currently exist for all cases [17].

In our cases, the location of the BA complex in the anterior half of the 3VF involved Class A (16 %) and Class B (12.8 %), resulting in a 28.8 % rate, while in the posterior half, which involves Class C (35.2 %) and Class D (36 %) were 71.2 %, and therefore, with our results, the axial "vascular safe zone" for fenestration is in the anterior half (Class A – B). Gangemi et al. found that the minimal width of the 3VF for safe endoscope maneuvers is estimated to be between 8 and 10 mm [22]. It is recommended that the fenestration stoma width should be at least 3–5 mm [4]. However, our results indicate a smaller mean lateral wall distance of the 3VF between the two hypothalamus, with a measure of 5.52 mm (SD: 1.5 mm). This difference raises important considerations regarding the applicability of the previously proposed empirical "safe zone criteria" to each patient population. Further research involving larger and more diverse patient cohorts would be valuable to refine our understanding of safe endoscope maneuvers within the third ventricle and optimize patient outcomes.

In our results, the top of the BA complex from the 3VF revealed that Type II was the most prevalent (74 %), followed by Type III (18.8 %) and Type I (7.2 %). These findings suggest that most patients had the top of the BA complex located within a range of 4 mm to 7.9 mm from the 3VF. This result correlates with Horsburgh et al.'s morphometric imaging analysis of MRI, which revealed that the mean distances from the 3VF to the BA top, right P1 segment, and left P1 segment were 4.9 mm, 5.5 mm, and 5.7 mm, respectively [23].

Aydin et al., in a classic neuroanatomical research, reported that the mean distance between the BA top and the center of the floor of 3VF was significantly greater in individuals without ventricular enlargement, measuring 6.54 ± 1.25 mm (mean ± SD). In contrast, individuals with ventricular enlargement had a reduced distance, averaging 2.75 ± 0.67 mm (mean ± SD). ($P < 0.001$) [24].

Guil-Ibáñez et al. and Kurucz et al. highlighted the dorsum sellae and the clival line as reliable anatomical landmarks for guiding floor perforation during endoscopic transsphenoidal surgery (ETVS). These neuroanatomical structures provide a "stable and reproducible" framework; the dorsum sellae and clival line enhance the neurosurgeon's ability to navigate the complex anatomy of the third ventricle safely [6,25].

Furthermore, midsagittal MRI views demonstrated that in 10 % of cases, the BA either made contact with or was within 1 mm of the undersurface of the 3VF [23,26]. This also correlates with our results, as Type I accounted for 7.2 %, indicating that the top of the BA is located at a distance of ≤4 mm from the 3VF.

Finally, Hayashi et al. conducted MRI-based research, revealing a mean distance of 12 ± 3.7 mm between the infundibular recess and the BA top. However, in elderly individuals, this distance can decrease to as little as 6 mm due to the anterior displacement of the BA relative to the mammillary bodies [26]. In our results, there was no significant correlation between age and the distance from the top of the BA to the 3VF.

4.1. Limitations

The study has several limitations that warrant consideration. Firstly, the sample size may not fully capture the diversity of the hydrocephalus population. The limited variation in patient demographics and hydrocephalus characteristics may restrict the generalizability of the findings to all patient groups.

Furthermore, the study relied exclusively on neuroradiological imaging to describe the position of the BA complex. This approach may overlook certain neuroanatomical and demographic variations that could be more visualized or confirmed using other techniques, such as neuroendoscopy intraoperative observations.

The study also did not evaluate clinical outcomes, such as postoperative complications or the success rates of surgical interventions

based on the proposed "vascular safe zone" for fenestration. Without this clinical correlation, it remains unclear whether the identified safe zone is universally applicable or if it needs to be adjusted based on individual patient characteristics.

5. Conclusions

Special attention should be directed towards preoperative MRI assessment, particularly focusing on the morphology of the 3VF. In our cases, the BA complex was located in the anterior half in 28.8 % of cases, with 16 % in Class A and 12.8 % in Class B. The remaining 71.2 % were located in the posterior half, with 35.2 % in Class C and 36 % in Class D. As a result, our findings suggest that the "vascular safe zone" for ETV fenestration in the axial classification is in the anterior half of the 3VF, represented by Classes A + B. The mean distance from the top of the BA complex to the 3VF was 6.86 mm (SD 1.56 mm). Further research should validate the "vascular safe zone" ETV fenestration considering patient demographics, presurgical clinical variables, and intraoperative BA complex lesions for evidence-based surgical planning.

Disclosure of funding or sponsorship

None.

CRediT authorship contribution statement

Nicolás Rincón-Arias: Writing – review & editing, Writing – original draft, Validation, Supervision, Methodology, Investigation, Conceptualization. **Nadin J. Abdala-Vargas:** Writing – review & editing, Formal analysis, Data curation, Conceptualization. **Sabino Luzzi:** Writing – review & editing, Writing – original draft, Validation, Supervision. **Julián D. Barraza:** Writing – review & editing, Writing – original draft, Validation, Conceptualization. **Luisa Fernanda Jaimes:** Writing – review & editing, Software, Resources, Methodology. **Pablo Baquero:** Visualization, Supervision, Resources, Data curation, Conceptualization. **Matias Baldoncini:** Writing – review & editing, Writing – original draft, Validation, Supervision. **Álvaro Campero:** Writing – review & editing, Writing – original draft, Validation, Supervision. **Daniela Martínez Laverde:** Writing – review & editing, Writing – original draft, Validation, Conceptualization. **Edgar G. Ordoñez-Rubiano:** Writing – review & editing, Validation, Supervision, Methodology, Conceptualization. **Hernando A. Cifuentes-Lobelo:** Writing – review & editing, Writing – original draft, Validation, Supervision, Resources.

Declaration of competing interest

The authors declare that they have no known competing financial interests or personal relationships that could have appeared to influence the work reported in this paper.

Illustrative cases:

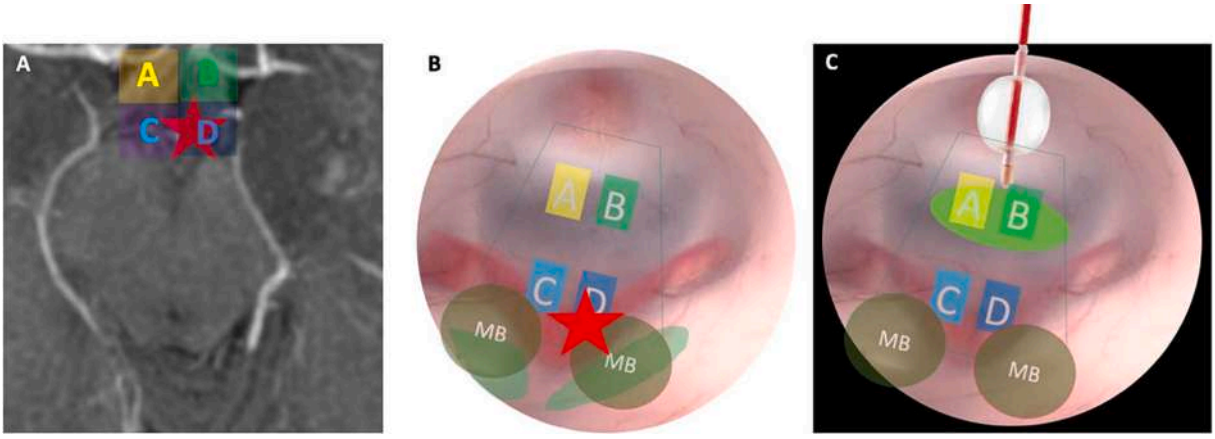

Illustrative case number 1: (**A**) T1-weighted MRI with contrast, that shows the top of the BA and BA complex in the D quadrant. (**B**) Endoscopic view during a ETV that shows the top of the BA and BA complex at the same location; the red star indicates the risk zone for iatrogenic arterial lesion. (**C**) The green circle marks the safe zone for fenestration in A – B quadrants. *MB: Mammillary bodies.*

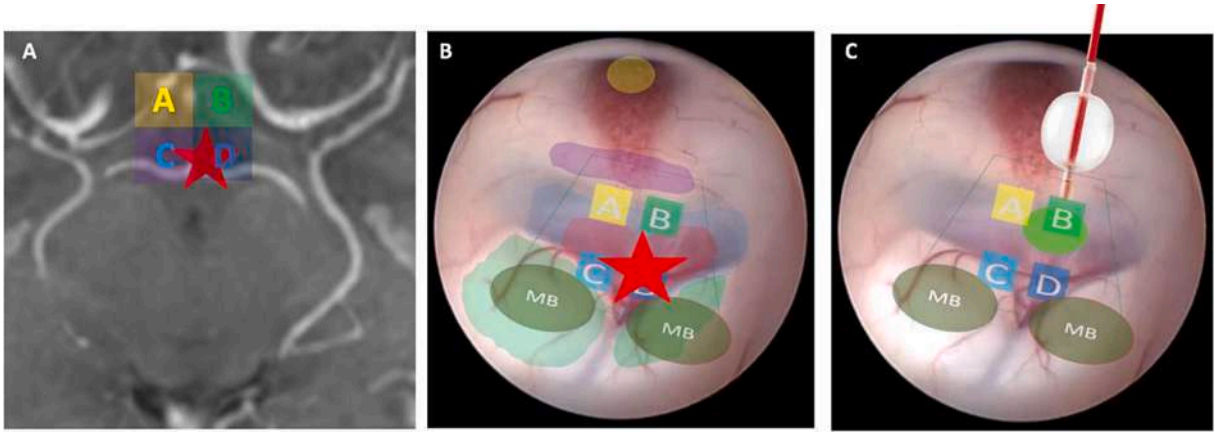

Illustrative case number 2: A similar case from case number 1. (**A**) T1-weighted MRI with contrast, that shows the top of the BA and BA complex in the D quadrant. (**B**) Endoscopic view during a ETV that shows the top of the BA and BA complex at the same location; the red star indicates the risk zone for iatrogenic arterial lesion. (**C**) The green circle marks the safe zone for fenestration in the B quadrant. *MB: Mammillary bodies.*

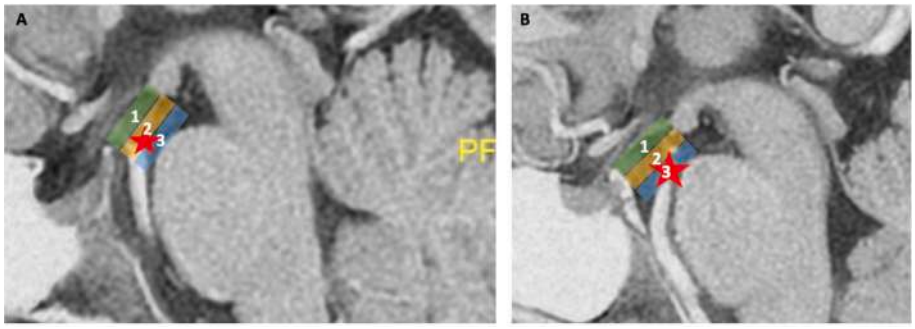

Illustrative cases numbers 3 - 4: (A) T1-weighted MRI with contrast, showing the top of the BA in the Type 2 position, with a distance between the third ventricle floor (3VF) and the top of the BA complex ranging from 4.1 mm to 8 mm. (**B**) T1-weighted MRI with contrast, showing the top of the BA in the type 3 position, with a distance between the 3VF and the top of the BA greater than 8 mm.

References

[1] Jiang L, Gao G, Zhou Y. Endoscopic third ventriculostomy and ventriculoperitoneal shunt for patients with noncommunicating hydrocephalus: a PRISMA-compliant meta-analysis. Medicine (Baltimore) 2018 Oct;97(42):e12139.

[2] Ernestus RI, Krüger K, Ernst S, Lackner K, Klug N. Relevance of magnetic resonance imaging for ventricular endoscopy. Minim Invasive Neurosurg MIN 2002 Jun;45 (2):72–7.

[3] Feng Z, Li Q, Gu J, Shen W. Update on endoscopic third ventriculostomy in children. Pediatr Neurosurg 2018;53(6):367–70.

[4] Stachura K, Grzywna E, Kwinta BM, Moskała MM. Endoscopic third ventriculostomy – effectiveness of the procedure for obstructive hydrocephalus with different etiology in adults. Wideochirurgia Inne Tech Maloinwazyjne Videosurgery Miniinvasive Tech 2014 Dec;9(4):586–95.

[5] Abdala-Vargas NJ, Cifuentes-Lobelo HA, Ordoñez-Rubiano E, Patiño-Gomez JG, Villalonga JF, Lucifero AG, et al. Anatomic variations of the floor of the third ventricle: surgical implications for endoscopic third ventriculostomy. Surg Neurol Int 2022;13:218.

[6] Guil-Ibáñez JJ, Gomar-Alba M, Castelló-Ruiz MJ, Saucedo L, Parrón-Carreño T, Castro-Luna GM, et al. An overview of the use of the dorsum sellae and clival line as a guide in endoscopic third ventriculostomy: historical, anatomical and technical aspects. Neurosurg Rev 2025 Mar 6;48(1):283.

[7] Rhoton AL. The lateral and third ventricles. Neurosurgery 2002;51(suppl_4):S1-207–1-271.

[8] Aydin S, Yilmazlar S, Aker S, Korfali E. Anatomy of the floor of the third ventricle in relation to endoscopic ventriculostomy. Clin Anat 2009;22(8):916–24.

[9] Fernandes-Silva J, Silva SM, Alves H, Andrade JP, Arantes M. Neurosurgical anatomy of the floor of the third ventricle and related vascular structures. Surg Radiol Anat SRA 2021 Dec;43(12):1915–25.

[10] Sughrue ME, Chiou J, Burks JD, Bonney PA, Teo C. Anatomic variations of the floor of the third ventricle: an endoscopic study. World Neurosurg 2016 Jun;90:211–27.

[11] Schmidt RH. Use of a microvascular Doppler probe to avoid basilar artery injury during endoscopic third ventriculostomy. Technical note. J Neurosurg 1999 Jan;90 (1):156–9.

[12] Grand W, Leonardo J, Chamczuk AJ, Korus AJ. Endoscopic third ventriculostomy in 250 adults with hydrocephalus: patient selection, outcomes, and complications. Neurosurgery 2016 Jan;78(1):109–19.

[13] Baykan N, Isbir O, Gerçek A, Dağçnar A, Ozek MM. Ten years of experience with pediatric neuroendoscopic third ventriculostomy: features and perioperative complications of 210 cases. J Neurosurg Anesthesiol 2005 Jan;17(1):33–7.

[14] Bouras T, Sgouros S. Complications of endoscopic third ventriculostomy: a systematic review. Acta Neurochir Suppl 2012;113:149–53.

[15] McLaughlin MR, Wahlig JB, Kaufmann AM, Albright AL. Traumatic basilar aneurysm after endoscopic third ventriculostomy: case report. Neurosurgery 1997 Dec;41(6):1400–3. discussion 1403–1404.

[16] Schroeder HW, Warzok RW, Assaf JA, Gaab MR. Fatal subarachnoid hemorrhage after endoscopic third ventriculostomy. Case report. J Neurosurg 1999 Jan;90(1): 153–5.

[17] Wasi MSI, Sharif S, Shaikh Y. Endoscopic third ventriculostomy: role of image guidance in reducing the complications. Asian J Neurosurg 2020;15(4):926–30.

[18] A novel protocol of continuous navigation guidance for endoscopic third ventriculostomy – PubMed [Internet]. [cited 2024 Apr 15]. Available from: https://pubmed.ncbi.nlm.nih.gov/25121792/.

[19] Yadav YR, Parihar VS, Ratre S, Kher Y. Avoiding complications in endoscopic third ventriculostomy. J Neurol Surg Part Cent Eur Neurosurg 2015 Nov;76(6):483–94.

[20] Peltier J, Fichten A, Page C, Havet E, Foulon P, Mertl P, et al. Endoscopic anatomy of the terminal portion of the basilar artery and its distal perforating branches. Morphol Bull Assoc Anat 2008 Mar;92(296):31–6.

[21] Romero ADCB, Aguiar PHP de, Borchartt TB, Conci A. Quantitative ventricular neuroendoscopy performed on the third ventriculostomy: anatomic study. Neurosurgery 2011 Jun;68(2 Suppl Operative):347–54; discussion 353–354.

[22] Gangemi M, Donati P, Maiuri F, Longatti P, Godano U, Mascari C. Endoscopic third ventriculostomy for hydrocephalus. Minim Invasive Neurosurg MIN 1999 Sep;42 (3):128–32.
[23] Horsburgh A, Matys T, Kirollos RW, Massoud TF. Tuber cinereum proximity to critical major arteries: a morphometric imaging analysis relevant to endoscopic third ventriculostomy. Acta Neurochir (Wien) [Internet]. 2013 May 1 [cited 2024 Apr 7];155(5):891–900. Available from: https://doi.org/10.1007/s00701-013-1661-9.
[24] Aydin S, Yilmazlar S, Aker S, Korfali E. Anatomy of the floor of the third ventricle in relation to endoscopic ventriculostomy. Clin Anat N Y N 2009 Nov;22(8): 916–24.
[25] Kurucz P, Barany L, Buchfelder M, Ganslandt O. The clival line as an important arachnoid landmark during endoscopic third ventriculostomy: an anatomic study. World Neurosurg 2018 Dec;120:e877–88.
[26] Hayashi N, Endo S, Hamada H, Shibata T, Fukuda O, Takaku A. Role of preoperative midsagittal magnetic resonance imaging in endoscopic third ventriculostomy. Minim Invasive Neurosurg MIN 1999 Jun;42(2):79–82.